Korean J. Chem. Eng., **29**(11), 1556-1566 (2012)
DOI: 10.1007/s11814-012-0035-y

Removal of Co, Sr and Cs from aqueous solution using self-assembled monolayers on mesoporous supports

Younjin Park, Won Sik Shin†, and Sang-June Choi

Department of Environmental Engineering, Kyungpook National University, Deagu 702-701, Korea
(*Received 1 November 2011 • accepted 10 March 2012*)

Abstract−Sorptive removal of Co, Sr and Cs from aqueous solution by SAMMS was investigated. The single-solute sorption data were well fitted by the Freundlich, Langmuir and Dubinin-Radushkevich models (R^2>0.95). The maximum sorption capacities (q_{mL}) of the Langmuir model were in the order of Cs (1.14 mmol/g)>Co (0.20 mmol/g)≈Sr (0.195 mmol/g). The bi-solute competitive sorption of the metals was analyzed by the Langmuir, competitive Langmuir, modified extended Langmuir and P-factor models. The sorption of one metal was suppressed by the presence of competing metals. Sorptions of Co and Sr were strongly dependent on the initial solution pH but that of Cs was not. The calculated thermodynamic parameters such as ΔH^0, ΔS^0 and ΔG^0 showed that sorption of Co onto SAMMS was endothermic, whereas those of Sr and Cs were exothermic. The negative ΔG^0 values indicated all the sorption processes were spontaneous in nature.

Key words: Cesium, Cobalt, Mesoporous Silica, Self-assembled Monolayers on Mesoporous Supports (SAMMS), Sorption, Strontium

INTRODUCTION

Silane-based self-assembled monolayers are valuable for chemically modifying surfaces for catalysis, chemical separation and sensing/detection. These monolayers are readily terminated with a wide variety of ligands, making them ideally suited for chelating transition metal species [1]. When this self-assembled monolayer chemistry is combined with mesoporous materials, a powerful new class of environmental sorbent material is obtained with high surface area (~1,000 m^2/g), easy chemical accessibility and high diffusion rates. These mesoporous hybrid materials, called self-assembled monolayers on mesoporous supports (SAMMS), are highly efficient sorbents whose interfacial chemistry can be tuned to selectively sequester specific species, such as heavy metals, tetrahedral oxometalate anions, and radionuclides [2]. The rigid, open pore structure of the mesoporous support makes all of the interfacial binding sites available to solution borne species and allows for facile diffusion into the porous matrix, resulting in rapid sorption kinetics [3].

For environmental applications, the functionalized mesoporous silicas with mercaptopropyl group, aminopropyl group, amine group and aminoethylaminopropyl group have been studied to remove heavy metals [4]. Liu et al. [5] synthesized a mercaptopropyl functionalized mesoporous silica (MCM-41) with a high sorption affinity for mercury (2.5 mmol/g). Liu et al. [6] prepared thiol- and amino-functionalized SBA-15 silicas and employed them for removing heavy metal ions from wastewater. The thiolated SBA-15 sorbent exhibited a higher complexation affinity for Hg^{2+}, while the other metal ions (Cu^{2+}, Zn^{2+}, Cr^{3+} and Ni^{2+}) showed exceptional binding ability with aminated analogue. Zhang et al. [7] applied multi-amine-grafted mesoporous silicas (SBA-15), which showed almost equal affinity to Hg^{2+}, Pb^{2+}, Zn^{2+}, Cu^{2+} and Cd^{2+} in wastewater. This can be attributed to both the large content of amino groups and the increased steric freedom and accessibility of the functional groups in the large pore channels of SBA-15. Mureseanu et al. [8] prepared N-propylalicylaldimino-functionalized SBA-15 mesoporous silica which showed high sorption capacity and selectivity of copper ion.

Several studies reported on the functional chelating groups attached on silica surface to remove Co, Sr and Cs from aqueous solution. Hanzel and Rajac [9] prepared silica gel and mesoporous silica (MCM-41) with covalent immobilized organofunctional groups (imidazole, diaza-18-crown-6) and evaluated Co sorption onto the sorbents. Lin et al. [10] synthesized copper ferrocyanide immobilized within a mesoporous silica matrix as a novel Cs sorbent. Chang et al. [11] also prepared nickel hexacyanoferrate multilayers on functionalized mesoporous silica supports for selective sorption and sensing of Cs. Sangvanich et al. [12] evaluated removal of cesium and thallium onto copper ferrocyanide on mesoporous silica from natural waters and simulated acidic and alkaline wastes. However, the previous studies did not investigate the influence of competing metal ions such as Co, Sr and Cs simultaneously existed in low-level radioactive wastewater from nuclear power plants.

The objective of this study is to investigate the applicability of SAMMS to remove Co, Sr and Cs from aqueous solution. The single- and bi-solute competitive sorptions of Co, Sr and Cs onto SAMMS were investigated and were fitted to several models such as Freundlich, Langmuir, Dubinin-Radushkevich (D-R) competitive Langmuir, modified extended Langmuir and P-Factor models. Effects of pH and temperature on the sorption mechanisms of Co, Sr and Cs were also investigated.

†To whom correspondence should be addressed.
E-mail: wshin@mail.knu.ac.kr

MATERIALS AND METHODS

1. Chemicals

The mesoporous silica (MCM-41 type) and ethylenediamine (EDA) terminated silane (N-[3-(trimethoxysilyl)propyl]-ethylenediamine, 97%) were purchased from Aldrich, Korea. The 2-propanol (99.5%) was provided by Duksan Chemicals Co., Korea. Copper chloride ($CuCl_2$, 97%) was from Junsei Chemical Co., Japan. Sodium ferrocyanide ($Na_4Fe(CN)_6$, 99%) was obtained from Riedel-deHaën, Germany. Cobalt nitrate ($Co(NO_3)_2 \cdot 6H_2O$, 98+%), strontium nitrate ($Sr(NO_3)_2$, 99+%) and cesium nitrate ($CsNO_3$, 99+%) were purchased from Sigma-Aldrich Chemical Co. (Milwakee, WI, USA). MES (2-[N-morpholino]ethanesulfonic acid hydrate, 99.5%) buffer was purchased from ACROS Organics (NJ, USA). All reagents were of analytical grade and were used without further purification.

2. The Sorbent Preparation

The SAMMS synthesis was based on the method proposed by Lin et al. [10]. Mesoporous silica (MCM-41 type) was first suspended in 60 mL toluene and treated with 0.7 mL distilled and deionized water (approximated two monolayer's worth of water). The addition of water caused immediate agglomeration of the silica, as indicated by the clumping of the previous dispersed powder. The mixture was then stirred vigorously for 2 hr at room temperature to allow the water to disperse throughout the mesoporous matrix. 3.4 mL of EDA terminated silane (one monolayer worth) was added into the mixture, and then the mixture was heated to reflux for 6 hr. Addition of the silane caused an immediate and noticeable reduction in the apparent viscosity of the slurry. During heating, the color of the mixture changed to a little yellow. At the end of reflux period, the reflux condenser was removed and replaced by a still head, and the methanol and water were removed via azeotropic distillation. This step is critical in the preparation of high-quality monolayer coatings because it drives the condensation equilibriums of monolayer formation to completion. After 20 min, all of the methanol and water were removed and then the mixture was cooled to room temperature. The product was collected by filtration through 1.2 μm cellulose nitrate membrane filter (Whatman), washed with 2-propanol and then air dried to obtain EDA-SAMMS.

The prepared functionalized silica was mixed with 60 mL of 0.25 M $CuCl_2$ solution and the mixture was stirred for 2 hr to obtain Cu-EDA-SAMMS. The product was collected by filtration through the membrane filter, washed with deionized water and 2-propanol and then air dried. The Cu-EDA-SAMMS still contains a significant number of anchoring and cross-linking defects. To cure these defects, the Cu-EDA-SAMMS was suspended in 60 mL toluene in a Dean-Stark apparatus and heated to reflux for 2 hr to drive the condensation of the dangling Si-OH groups. Thereafter, the mixture was cooled to room temperature and the product was collected by filtration through the membrane filter, washed thoroughly with 2-propanol and then air dried to obtain little blue color powder. Finally, Cu-EDA-SAMMS (2.0 g) was converted to the hexacyanoferrate form by shaking with 50 mL of 0.25 M $Na_4Fe(CN)_6$ for 1 hr. The product was filtered through the membrane filter and washed with deionized water and air dried to obtain reddish brown powder.

3. Characterization of the Sorbent

The physicochemical properties of the sorbent were investigated. Specific surface area was determined by fitting the Brunauer-Emmett-Teller (BET) model to the N_2 sorption/desorption isotherm. The pore size distribution, pore volume and pore diameter (micro-, meso-, and/or macro-pores) were determined by Barrett-Joyner-Halenda (BJH) sorption model using specific surface area analyzer (UPA-150, Microtrac, USA). Scanning electron microscopy (SEM, S-4200, HITACHI, Japan) with energy dispersive X-ray (EDX, Horiba, E-MAX EDS detector) analyses were conducted to study surface morphology and chemical composition of the sorbent. The transmission electron microscopy (TEM) images were taken using a JEM-2010 (JEOL, Japan). The samples were prepared by ultrasonic dispersion, using absolute alcohol as a solvent and micro-grid as a support membrane. X-ray diffraction (XRD) patterns were obtained using Cu Kα radiation (λ=1.54 Å) on multi-purpose x-ray diffractometer (X'pert PRO MRD, PANalytical, Netherlands). XRD peaks data for wide angle from 2° to 50° of 2θ were measured with a step size of 0.02 and a step time of 1.5 s and for short angle from 1.5° to 6.5° of 2θ were measured with a step size of 0.01 and a step time of 4 s. The pH of point of zero charge (pH_{PZC}) of the sorbent was determined by batch technique. 0.2 g of SAMMS with 30 mL of 0.1 M KNO_3 solution as an inert electrolyte was mixed in 50 mL conical tubes (Polyethylene, SPL Co., Korea). The initial pH (from 2 to 10) of the solution was adjusted by adding 0.1 N HNO_3 or 0.1 N KOH. The samples were shaken for 24 hr at 200 rpm and 25 °C to reach equilibrium. The final pH of the solution was measured by pH meter (720 A+, Thermo Orion, USA).

4. Sorption Experiment

Single-solute sorption experiments were conducted using 15 mL conical tubes containing 0.1 g of the sorbent. The pH of the sorbent was controlled to 5 by rinsing the sorbent two times with 0.05 M MES buffer solution before performing all experiments. The tubes containing the sorbent were filled with metal solutions and the headspace was minimized to exclude the effect of carbon dioxide in the air. Then, the vials were placed on a shaking incubator and mixed for 24 hr at 20 °C and 200 rpm. To obtain sorption isotherm, metal solutions with six to seven different initial concentrations (1, 2, 5, 10, 15 and 20 or 30 mM) of Co, Sr and Cs were prepared. The pH of the metal solution was also controlled to 5 using 0.05 M MES buffer. Preliminary experiments showed that the buffer has no effect on metal sorption. Wolff-Boenisch and Traina [13] also reported that no detectable complexation reactions occurred between metals and MES buffer. After sorption experiments, the vials were centrifuged and the supernatant was filtered through 0.2 μm cellulose nitrate membrane filter (Whatman). The aqueous phase concentrations of the metals were analyzed by inductively coupled plasma-optical emission spectrometry (ICP-OES, Optima 2100 DV, Perkin-Elmer Co., USA). The concentrations of Cs were analyzed by standard addition method [14]. The solid phase equilibrium concentrations were calculated from the mass balance by assuming that all concentration changes in solution phase resulted from sorption onto the solid phase.

Bi-solute systems (Co/Sr, Sr/Cs and Co/Cs) were prepared by mixing each metal solution of the same molar concentration (1-20 mM) in a 1 : 1 volume ratio. Bi-solute competitive sorption experiments were conducted in the same manner as were in the single-solute sorption experiments. The aqueous phase concentrations of the metals in the mixture were analyzed by ICP-OES.

5. Sorption Models

The Freundlich, Langmuir and Dubinin-Radushkevich (D-R)

models were applied to explain the sorption mechanism of the metals onto the sorbent in single-solute system.

The Freundlich model is often used to describe sorption onto heterogeneous surface:

$$q = K_F C^{N_F} \quad (1)$$

where C (mmol/L) is the aqueous-phase equilibrium concentration, q (mmol/g) is the solid-phase equilibrium concentration, and K_F [(mmol/g)/(mmol/L)^N] and N_F (−) are the Freundlich sorption coefficient and the Freundlich exponent, respectively.

The Langmuir model is described by a limiting maximum sorption capacity that is related to monolayer coverage of surface sites:

$$q = \frac{q_{mL} b_L C}{1 + b_L C} \quad (2)$$

where q_{mL} (mmol/g) and b_L (L/mmol) are the Langmuir parameters representing maximum sorption capacity and site energy factor, respectively.

The Dubinin-Radushkevich isotherm (D-R) is more general than the Langmuir isotherm because it does not assume a homogeneous surface or constant sorption potential [15]. The D-R isotherm is applied to distinguish between physical and chemical sorptions.

$$q = q_{mD}\exp(-\beta\varepsilon^2) = q_{mD}\exp\left[-\beta\left(RT\ln\left(1+\frac{1}{C}\right)\right)^2\right] \quad (3)$$

where β is a constant related to the mean free energy of sorption per mole of the sorbate (mmol^2/J^2), q_{mD} is the theoretical saturation capacity (mmol/g) and ε is the Polanyi potential, which is equal to RTln(1+1/C), where R (J/mol-K) is the gas constant and T (K) is the absolute temperature. The constant β gives an idea about the mean free energy E (J/mol) of the sorption per molecule of the sorbate when it is transferred to the surface of the solid from infinity in the solution and this energy can be computed by using the following relationship [15].

$$E = \frac{1}{(2\beta)^{1/2}} \quad (4)$$

The sorption model parameters were determined by using a commercial software package, Table Curve 2D® (Version 5.1, SYSTAT Software, Inc.).

The competitive Langmuir, the modified extended Langmuir and the P-Factor models were applied to explain the sorption mechanism of the metals onto the sorbent in bi-solute systems.

The competitive Langmuir model (CLM) was used to analyze bi-solute competitive sorption behaviors [16]. The CLM is an extended form of the Langmuir model which allows predictions of the amount of a solute *i* sorbed per unit weight of a sorbent, q_i in the presence of other solutes.

$$q_i = \frac{b_{L,i} q_{mL,i} C_i}{1 + \sum_{j=1}^{2} b_{L,j} C_j} \quad (5)$$

where q_i (mmol/g) and C_i (mmol/L) are the solid-phase and the liquid-phase concentration of a solute *i* in bi-solute competitive sorption, respectively. $q_{mL,i}$ (mmol/g) and $b_{L,i}$ (L/mmol) are the parameters determined by fitting the Langmuir model to the single-solute sorption data of solute *i*.

The modified extended Langmuir model (MELM) was derived from the extended Langmuir model (ELM) for analysis of the multi-solute sorption, where the synergistic or antagonistic efficiency (θ) of sorbates is introduced [17,18]. This efficiency is linearly related to the amount sorbed at equilibrium of the other solute.

$$\theta_i = a_i q_j + b_i \quad (i=1 \text{ or } 2) \quad (6)$$

where a_i and b_i are the constants parameters of synergistic efficiency and estimated from bi-solute competitive sorption data by non-linear regression. If $\theta_i > 0$, the sorbed amount of one solute (q_i) linearly increases with the sorbed amount of the other solute (q_j) (i.e., synergistic effect). If $\theta_i < 0$, sorption of one solute decreases by the presence of the other solute (i.e., antagonistic effect). The cross-over point of the two behaviors is $q_{j,cross} = b_i/a_i$ at $\theta_i = 0$.

The MELM is defined as:

$$q_i = \frac{b_{L,i} q_{mL,i} C_i}{1 + \sum_{j=1}^{N} b_{L,j} C_j}(1+\theta_i) \quad (i=1 \text{ or } 2) \quad (7)$$

If $\theta_i = 0$, the MELM becomes competitive Langmuir model (CLM). A FORTRAN program was written to estimate the MELM model parameters. The programs calls the IMSL subroutine ZXSSQ, which is based on a finite difference, Levenberg-Marquardt algorithm for solving nonlinear least squares problems.

The P-factor model was used to analyze bi-solute competitive sorption behaviors. This model is based on a simplified approach that can be used to compare and correlate single-solute sorptions with those of the multi-component systems by introducing a "lumped" capacity factor P_i [18]:

$$P_i = \frac{q_{mL,i}}{q^*_{mL,i}} \quad (8)$$

where $q_{mL,i}$ is the sorbent monolayer capacity for component *i* in single-solute component system, while $q^*_{mL,i}$ is that in bi-solute component system. This model assumes a Langmuir isotherm; hence, for each component *i*, the bi-component isotherm equation is described as:

$$q_i = \frac{1}{P_i}\frac{b_{L,i} q_{mL,i} C_i}{1 + b_{L,i} C_i} \quad (9)$$

6. Effect of pH

To investigate the effect of pH on the sorption, pH was adjusted to 2-12 using 0.1 N HNO_3 and 0.1 N NaOH. The vials containing 0.2 g of SAMMS were filled with 30 mL of 10 mM of Co, Cs and Sr solutions at different pHs. Sorption experiment was conducted as was in the single-solute sorption. After sorption, the supernatant was filtered through a 0.2 μm syringe filter (cellulose nitrate membrane filter, Whatman) and then analyzed for final pH and metal ion concentration. To determine the effect of pH on metal precipitation, the pH of 10 mM of sorbent-free metal solutions was adjusted to 2-12. After the suspensions were mixed for 24 hr at 20 ºC and 200 rpm, filtered through the syringe filter and then and analyzed for final pH and metal ion concentration. The aqueous phase concentrations of Co, Sr and Cs in the pH-adjusted solution were determined by the ICP-OES. The precipitated amount was calculated from the mass balance.

7. Effect of Temperature

The effect of temperature on the sorption of 10 mM of Co, Sr and Cs onto the sorbent was conducted at 283 K, 293 K and 313 K in the same manner as was in the single-solute sorption experiments.

The thermodynamic parameters for the sorption process, ΔH^0, ΔS^0 and ΔG^0 can be calculated using the following equations [19]:

$$K_d = \frac{q}{C} \tag{10}$$

$$\Delta G^0 = -RT\ln K_d \tag{11}$$

$$\Delta G^0 = \Delta H^0 - T\Delta S^0 \tag{12}$$

These three equations can be expressed as:

$$\ln K_d = \frac{\Delta S^0}{R} - \frac{\Delta H^0}{RT} \tag{13}$$

where ΔS^0 (J/mol/K) and ΔH^0 (J/mol) are the changes in the entropy and enthalpy for the sorption process, respectively, K_d (mL/g) is the distribution coefficient, T is the absolute temperature (K), and R is the gas constant (8.314 J/mol/K). The plot of ln K_d versus 1/T is linear with the slope and the intercept which give the values of ΔH^0 and ΔS^0, respectively.

RESULTS AND DISCUSSION

1. Sorbent Characteristics

The specific surface area (SSA), pore volume and pore size of MCM-41 and SAMMS are listed in Table 1. The surface area of MCM-41 highly decreased from 1,140 m^2/g to 14.27 m^2/g after grafting with functional ligands. The pore size decreased from 27.57 Å to 16.45 Å indicating monolayer functional ligands formation in mesopore surface. The surface area and pore size of SAMMS depending upon the degree of the functional group's coverage onto MCM-41 were reduced as the functional group grafted onto MCM-41.

SEM images of MCM-41 and SAMMS are presented in Fig. 1. The SEM image of MCM-41 (Fig. 1(a)) exhibits agglomerated particles and that of SAMMS (Fig. 1(b)) reveals that SAMMS has truncated bi-pyramid crystal morphology. The SEM image of SAMMS shows that the largest crystals in the population did not exceed 1.5 μm in length. Such small particle size has positive influence on the sorption of heavy metal ions. In the EDS analysis (Fig. 1(c)), the elemental atomic composition of SAMMS was 1.82% of Na, 4.72% of Cu and 1.63% of Fe and so on. According to this, the composition of sodium copper ferrocyanide immobilized on MCM-41 is $Na_{1.1}Cu_{2.9}Fe(CN)_6$ which is different with the one ($Na_{1.3}Cu_{1.5}Fe(CN)_6$) reported by Lin et al. [10]. This discrepancy may be dependent on the different synthesis conditions.

The TEM images of MCM-41 and SAMMS are presented in Fig. 2. The hexagonal pores arranged in an orderly manner as shown in the image of MCM-41 (Fig. 2(a)) were scarcely observed for

Table 1. Surface area, pore volume and pore size of the sorbent

	Surface area (m^2/g)	Pore volume (cm^3/g)	Pore size (Å)
MCM-41	1140	1.209	27.57
SAMMS	14.27	0.089	16.45

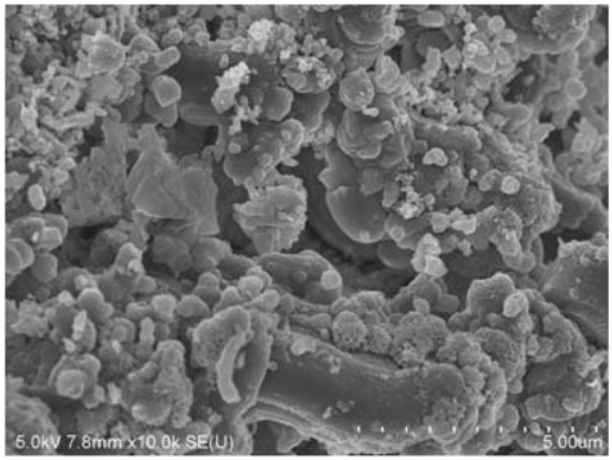

(a) MCM-41

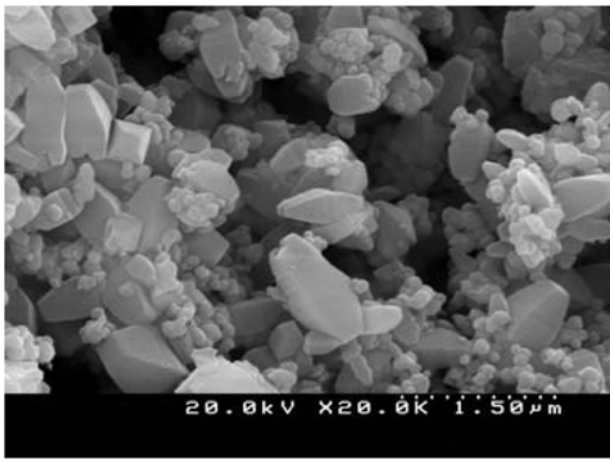

(b) SAMMS

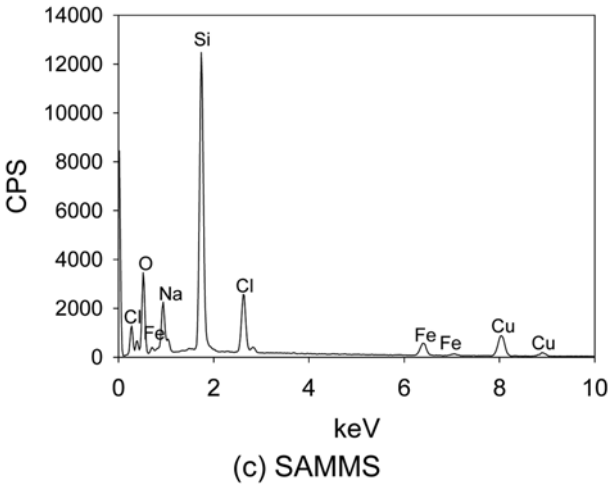

(c) SAMMS

Fig. 1. SEM images of (a) MCM-41 and (b) SAMMS and (c) EDS analysis of SAMMS.

SAMMS (Fig. 2(b)), which demonstrates that the order of MCM-41 was mostly destroyed after introducing functional group deposited on the surface of mesoporous MCM-41 and thus SAMMS might form some larger aggregates.

The XRD patterns of MCM-41 and SAMMS are illustrated in Fig. 3. The XRD peaks of SAMMS are considerably different from

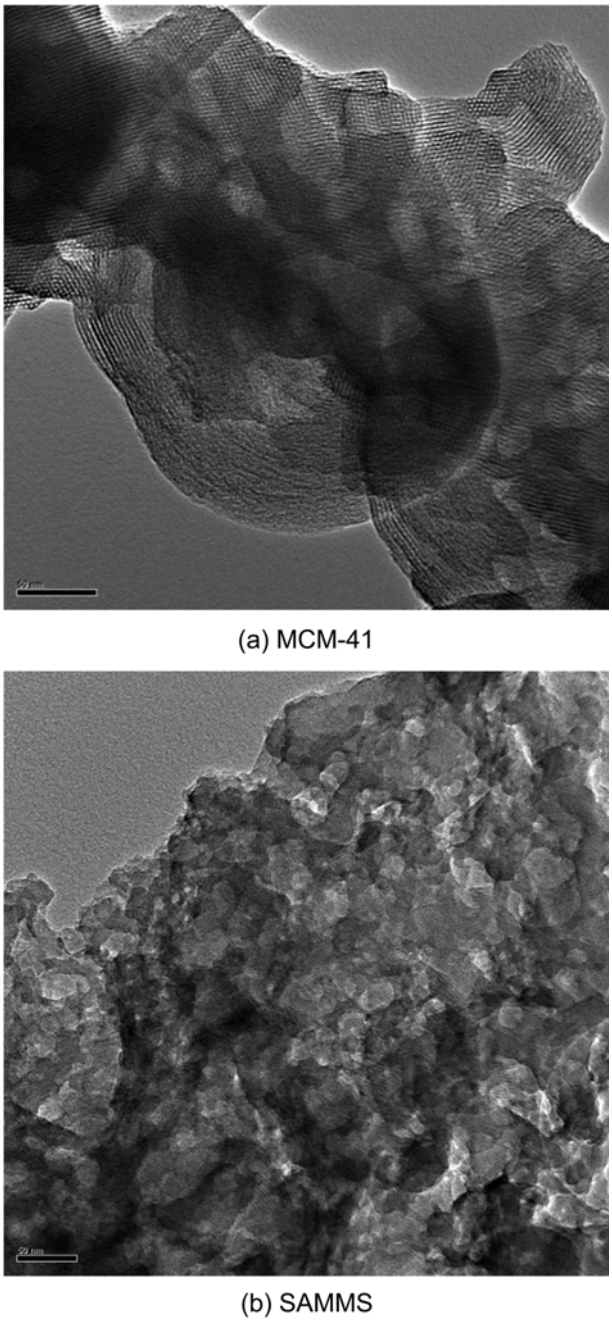

Fig. 2. TEM images of (a) MCM-41 and (b) SAMMS.

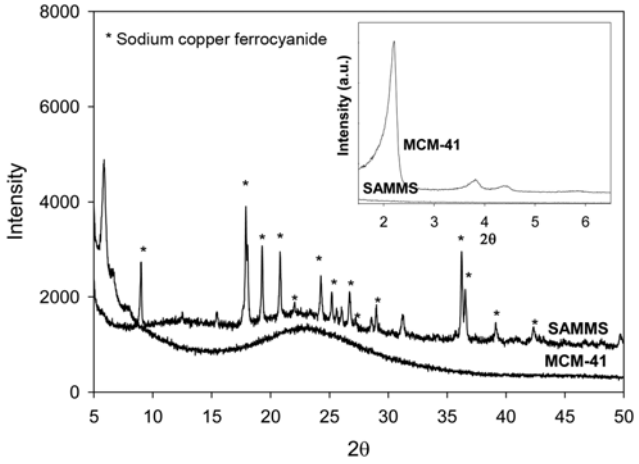

Fig. 3. XRD patterns of MCM-41 and SAMMS.

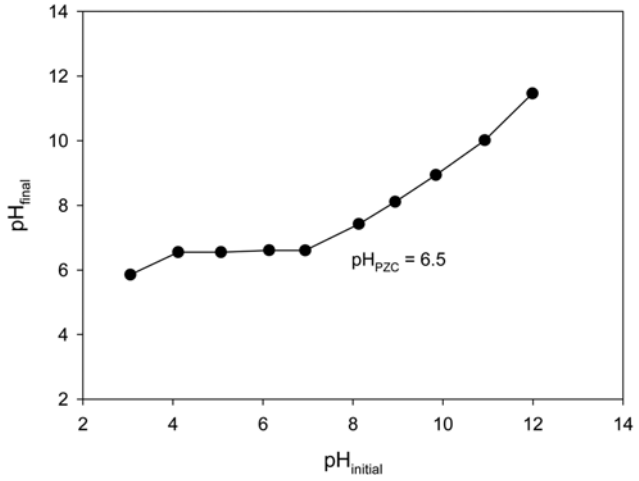

Fig. 4. The pH_{PZC} value determination of SAMMS.

that of MCM-41. The well-defined peaks of SAMMS in wide angle indicate that sodium copper ferrocyanide. Although the calculated structure of sodium copper ferrocyanide could not be exactly assigned by the JCPDS card due to changes of intensity and sharpness resulted from grafting organics onto MCM-41, the material was a class of ferrocyanide compounds of which metal atoms are linked by cyanide units [11]. XRD pattern in small angle indicates that MCM-41 has a typical hexagonal structure, showing a pattern featuring one main reflection at 2.19° and three weak reflections at 3.81°, 4.39°, and 5.83° corresponding to diffraction planes that could be indexed as 100, 110, 200, and 210, respectively. Compared with the XRD spectrum of MCM-41, SAMMS had quite lower intensity of the corresponding peak showing the lattice contraction of pore structure due to grafting organics, in agreement with TEM analysis. The pH_{PZC} value of SAMMS was 6.5 (Fig. 4). All sorption experiments were performed at pH 5, which means the negative surface charge of SAMMS surface was favorable on metal sorption.

2. Single-solute Sorption

Molar distributions of cobalt, strontium and cesium species at all pH ranges predicted by MINEQL+ (version 4.5) for Windows (Environmental Research Software, USA) are presented in Fig. 5. $Co(OH)_2$ was formed at pH>7 and $SrOH^+$ was formed at pH>11. Co^{2+}, Sr^{2+} and Cs^+ are the predominating species at pH 5 which was higher than the pH_{pzc} of SAMMS (=6.5), resulting in favorable sorption of the metal ions.

The single-solute sorptions of Co, Sr and Cs onto SAMMS are shown in Fig. 6 and the model parameters are summarized in Table 2. The sorption of metal ion increased with increasing initial metal ion concentration (C_0). This is attributed to the increase of driving force arising from the concentration gradient. The sorption capacity was in the order of Cs>Co>Sr.

The Freundlich, Langmuir, D-R models were fitted to the sorption data. The Freundlich model fitted the sorption data very well (R^2>0.98) (Table 2). The Freundlich sorption constant, K_F, indi-

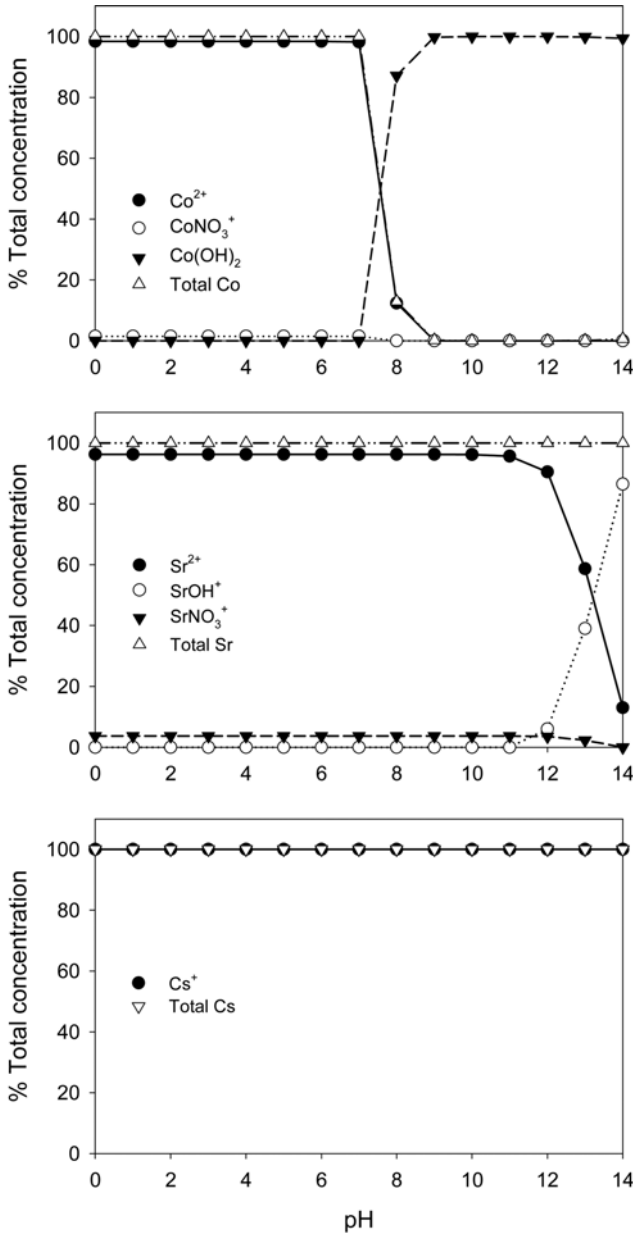

Fig. 5. % total concentrations of (a) Co, (b) Sr and (c) Cs species at different pH levels.

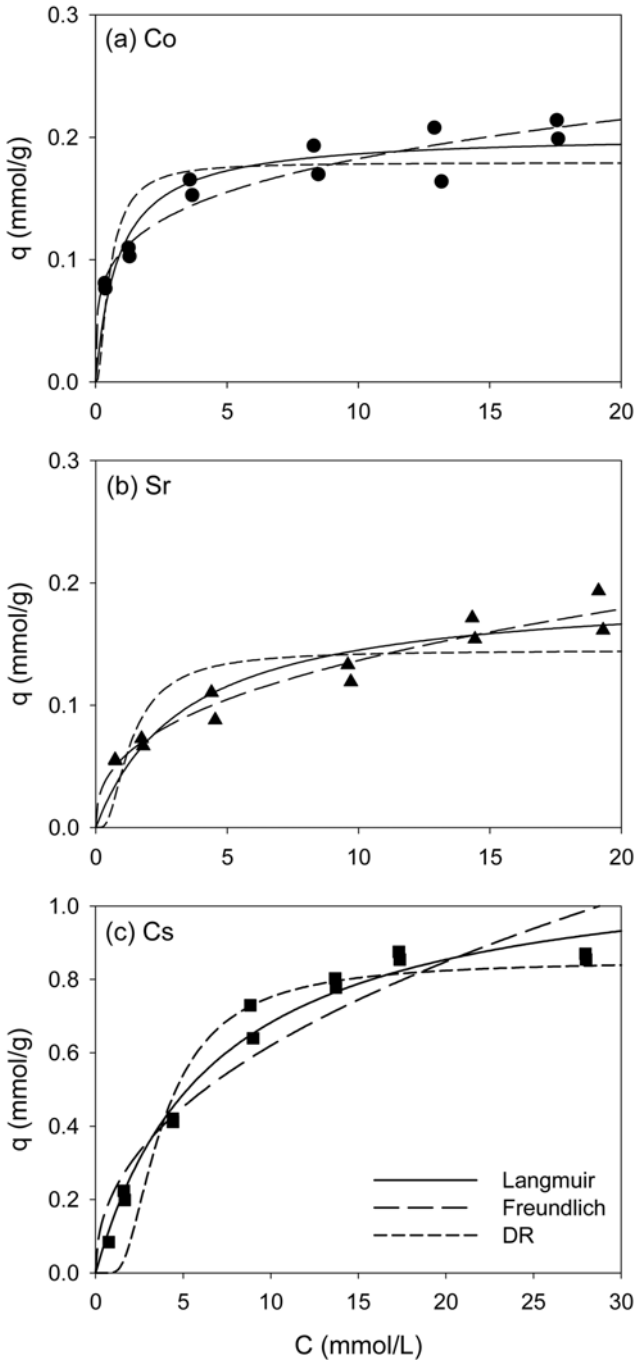

Fig. 6. Single-solute sorption of (a) Co, (b) Sr and (c) Cs onto SAMMS. Lines represent sorption models.

cates the sorption capacity of the sorbent. The K_F values were in the order of Cs>Co>Sr. The Freundlich exponent, N_F, is a measure of the derivation from linearity of the sorption. If a value for N_F is equal to unity, the sorption is linear. If N_F value is above 1, this implies that sorption process is chemical, but if N_F value is below 1, sorption is favorable for a physical process. The N_F values of the sorbent at equilibrium ranged between 0.23-0.45 represented that sorption was favorable and highly non-linear [20].

The Langmuir model also fitted the sorption data well (R^2>0.98) (Table 2). The maximum sorption capacity (q_{mL}) of SAMMS was in the order of Cs (1.141 mmol/g)>Co (0.203 mmol/g)≈Sr (0.195 mmol/g). The q_{mL} values indicate that SAMMS has a higher affinity for Cs than Co and Sr. Lin et al. [10] reported that the q_{mL} value of Cs on Cu-Ferrocyanide-EDA SAMMS was 1.33 mmol/g was higher than our result. This is due to the difference of the structural formula between the materials.

The fundamental characteristic of Langmuir isotherm can be expressed in terms of a dimensionless constant, separation factor K_R (−), that describes the type of isotherm [20].

$$K_R = \frac{1}{1 + b_L C_0} \tag{14}$$

where b_L is the Langmuir constant and C_0 is the initial concentration of heavy metal solution. The value of K_R indicates the type of

Table 2. Sorption model parameters for single-solute sorption of Co, Sr and Cs onto SAMMS

	Freundlich			
	K_F [(mmol/g)/(mmol/L)^{N_F}]	N_F (−)	R^2	SSE
Co	0.1067±0.0066	0.2334±0.0273	0.9923	0.0023
Sr	0.0562±0.0050	0.3860±0.0355	0.9925	0.0013
Cs	0.2181±0.0338	0.4533±0.0555	0.9809	0.1075
	Langmuir			
	q_{mL} (mmol/g)	b_L (L/mmol)	R^2	SSE
Co	0.2028±0.0091	1.1484±0.2664	0.9900	0.0031
Sr	0.1950±0.0168	0.2908±0.0844	0.9828	0.0032
Cs	1.1405±0.0554	0.1490±0.0207	0.9957	0.0241
	D-R			
	q_{mD} (mmol/g)	β (mol^2/J^2)	E (kJ/mol)	R^2	SSE
Co	0.1793±0.0095	2.23E-06	0.47	0.9764	0.0072
Sr	0.1448±0.0115	1.03E-07	2.20	0.9500	0.0092
Cs	0.8513±0.0395	3.82E-07	1.14	0.9825	0.0981

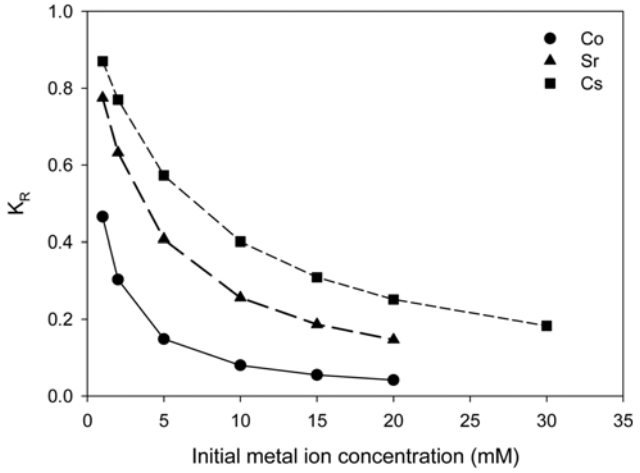

Fig. 7. Separation factors K_R for the sorption of Co, Sr and Cs onto SAMMS.

isotherm to be unfavorable (K_R>1), linear (K_R=1), favorable (0< K_R<1) or irreversible (K_R=0) [21]. The plot of separation factor K_R against initial metal ion concentration is shown in Fig. 7. The sorptions of all metal ions onto SAMMS were found to be favorable, and the sorption of metal ions at higher initial metal ion concentration was more favorable than that at lower initial metal ion concentration. The sorption of Co was the most favorable, although having relatively lower sorption capacity.

The Dubinin-Radushkevich (D-R) model parameters are listed in Table 2. The D-R model also fitted the sorption data well (R^2> 0.95). The order of increase in q_{mD} values was the same as the q_{mL} values of Langmuir model (Table 2), although the q_{mD} values were a little lower than the q_{mL} values. The difference is attributed to the different definition of q_m in the two models. In the Langmuir model, q_{mL} represents the maximum sorption capacity of metal ions at monolayer coverage, while q_{mD} represents that at the total specific micropore volume of the sorbent in D-R model [22]. The value of mean free energy E in D-R model indicates whether sorption mechanism is ion-exchange or physical sorption. If the E is between 8 and 16 kJ/mol, the sorption system progresses by ion-exchange, while for the value of E<8 kJ/mol, the sorption system is of a physical nature. For the value of E>16 kJ/mol, the sorption occurs by means of chemical sorption [15]. In this study, the E values calculated from Eq. (4) were less than 8 kJ/mol, indicating that sorption of Co, Sr and Cs on the sorbent followed physical sorption. The Freundlich exponent, N_F, in Freundlich model as well as the mean free energy E, in D-R model indicated that the mechanism of sorption was physical.

In conclusion, the metal sorption onto SAMMS could explain ion exchange as well as a further mechanism, such as chemical and/

Table 3. Langmuir model parameters for bi-solute competitive sorption of metal ions onto SAMMS

Binary system	Metal	q^*_{mL}	b^*_L	R^2	SSE
Co/Sr	Co	0.1879±0.0116	1.5806±0.5444	0.7401	0.0059
	Sr	0.0370±0.0022	1.6699±0.6398	0.5757	0.0002
Sr/Cs	Sr	0.1968±0.0468	0.1675±0.1069	0.7103	0.0099
	Cs	0.7598±0.0739	1.7922±1.1632	0.7418	0.1954
Co/Cs	Co	0.3055±0.0344	1.1846±0.0568	0.9124	0.0054
	Cs	0.3189±0.0326	2.1304±1.4977	0.1477	0.0483

q^*_{mL} (mmol/g) and b^*_L (L/mmol) denote Langmuir model parameters for bi-solute competitive sorptions

or physical sorption [23]. The dominant mechanism is ion exchange of the alkaline cations into the interstitial sites of Na-ferrocaynide in order to balance the permanent net negative charge on the matrix [11]. This is the reason why Cs sorption onto SAMMS was higher than Co or Sr sorption. The secondary mechanism is both chemical and electrostatic binding reaction. The surface hydroxyl groups of the silica matrix adsorb the metal ions in a relatively non-selective manner and electrostatic binding reaction between the metal ions and the negatively charged sites on SAMMS [11].

3. Bi-solute Competitive Sorption

Bi-solute competitive sorptions of Co/Sr, Co/Cs and Sr/Cs onto the sorbent were analyzed by the Langmuir model (Table 3). The maximum sorption capacity (q^*_{mL}) and sorption affinity (b^*_L) in bi-solute system were compared with those in single-solute system (q_{mL} and b_L). The q^*_{mL} of bi-solute competitive sorption (Table 3) was less than the q_{mL} of single-solute sorption (Table 2) as expected by the coexistence of competing metal ion.

The effect of bi-solute competition on the sorption of the metals was also analyzed by the ratios of the sorption capacity of one metal in the presence of other metal, q^*_{mL}, to the sorption capacity of corresponding metal in single-solute solution, q_{mL}, as summarized in Table 4. The $q_{mL,Co}/q_{mL,Sr}$ and $q^*_{mL,Co}/q^*_{mL,Sr}$ ratios were higher than unity, indicating the predominant sorption of Co in Co/Sr system onto the sorbent regardless of competition. However, the $q_{mL,Sr}/q_{mL,Cs}$ and $q^*_{mL,Sr}/q^*_{mL,Cs}$ ratios as well as the $q_{mL,Co}/q_{mL,Cs}$ and $q^*_{mL,Co}/q^*_{mL,Cs}$ ratios were lower than unity. It means that the Cs sorption onto SAMMS in single- or bi-solute system (with Co or Sr) is predominant. Most of the q^*_{mL}/q_{mL} ratios were lower than or equal to unity (Sr in Sr/Cs system) except Co in Co/Cs system. This means that the sorption was hindered by the presence of the other competing metals. In Co in Co/Cs system, the Co sorption was more promoted by the presence of Cs.

The bonding energy coefficients (b_L for single-solute sorption and b^*_L for bi-solute competitive sorption) varied with the relative affinity of the metal compared to the competing metals. The $b_{L,1}/b_{L,2}$ ratios of all Co/Sr, Sr/Cs and Co/Cs systems in single-solute sorption were higher than unity, indicating Co in Co/Sr, Sr in Sr/Cs and Co in Co/Cs sorbed more strongly onto the specific sorption sites of SAMMS. However, the $b^*_{L,1}/b^*_{L,2}$ ratios of all Co/Sr, Sr/Cs and Co/Cs systems in bi-solute sorption were lower than unity. It means that specific sorption of Co in Co/Sr, Sr in Sr/Cs and Co in Co/Cs was inhibited by competition. Especially, the $b^*_{L,Sr}/b^*_{L,Cs}$ and $b^*_{L,Co}/b^*_{L,Cs}$ the ratios were lower than 0.1, indicating the Sr and Co had weak sorption affinity than Cs due to competition. That was also confirmed through the b^*_L/b_L in Sr/Cs and Co/Cs sys- tem. The $b^*_{L,Sr}/b_{L,Sr}$ ratio (=0.58) was lower than unity, while the $b^*_{L,Cs}/b_{L,Cs}$ ratio (12.0) was much higher than unity in Sr/Cs system. The $b^*_{L,Co}/b_{L,Co}$ ratio (=0.16) was also lower than unity, while the $b^*_{L,Cs}/b_{L,Cs}$ ratio (=14.3) was also much higher than unity in Co/Cs system.

Competitive Langmuir model (CLM), modified extended Lang-

Table 4. Comparison of q_{mL} and b_L values of single- and bi-solute competitive sorption

Binary system (1)/(2)[a]	$q_{mL,1}/q_{mL,2}$	$q^*_{mL,1}/q^*_{mL,2}$	$q^*_{mL,1}/q_{mL,1}$	$q^*_{mL,2}/q_{mL,2}$
Co/Sr	1.0397	5.0764	0.9265	0.1898
Sr/Cs	0.1711	0.2590	1.0088	0.6662
Co/Cs	0.1779	0.9581	1.5063	0.2796
Binary system (1)/(2)[a]	$b_{L,1}/b_{L,2}$	$b^*_{L,1}/b^*_{L,2}$	$b^*_{L,1}/b_{L,1}$	$b^*_{L,2}/b_{L,2}$
Co/Sr	3.9504	0.9465	1.3784	5.6085
Sr/Cs	1.9483	0.0935	0.5770	12.034
Co/Cs	7.6965	0.0866	0.1609	14.306

q_{mL} and b_L values indicate Langmuir model parameters for single-solute sorption. q^*_{mL} and b^*_L indicate Langmuir model parameters for bi-solute competitive sorption. The metal in bi-solute competitive systems were labeled in the order of (1) and (2)

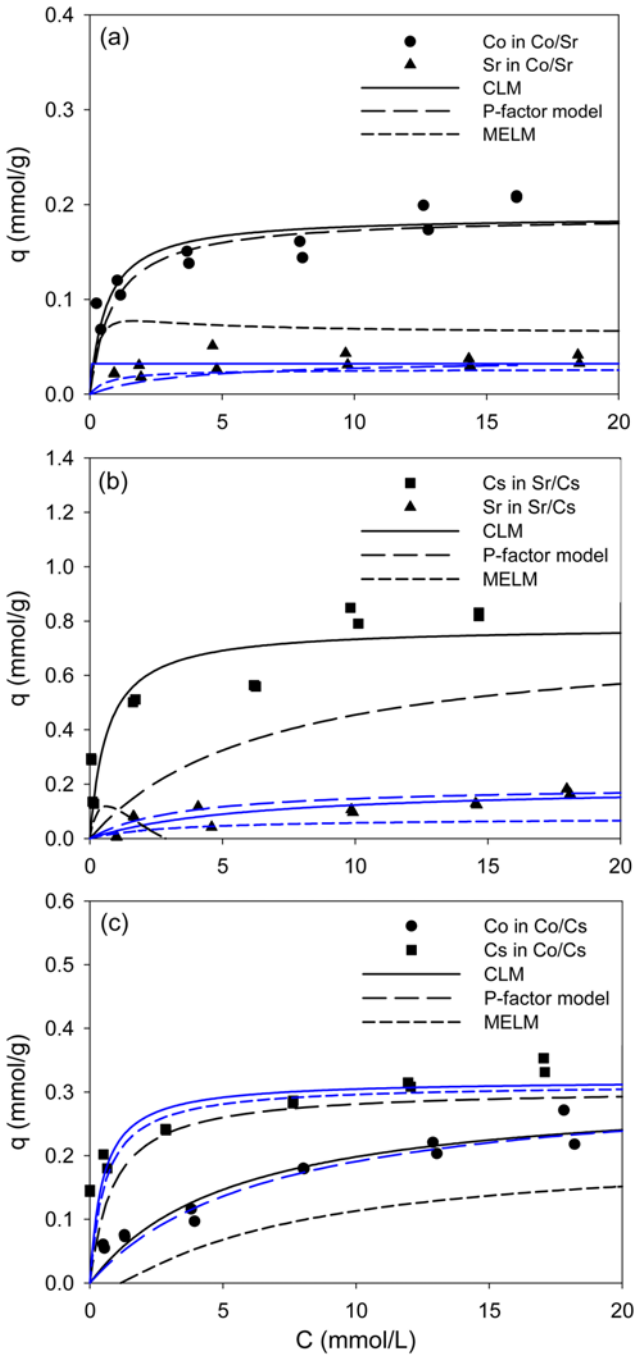

Fig. 8. Bi-solute competitive sorption of (a) Co/Sr, (b) Sr/Cs and (c) Co/Cs onto SAMMS. Lines represent competitive sorption models.

Table 5. R^2 and SSE values for bi-solute competitive sorption onto SAMMS predicted by competitive Langmuir model (CLM)

Binary system	R^2	SSE
Co/Sr	0.9690/0.9769	0.0183/0.0046
Sr/Cs	0.9491/0.7969	0.0166/1.9653
Cs/Co	0.9383/0.9552	0.3976/0.0279

muir model (MELM) and P-factor model (Fig. 8 and Tables 5-7) were also applied to explain the bi-solute competitive sorptions of Co/Sr, Sr/Cs and Co/Cs onto the sorbent. The coefficient of determination (R^2), the sum of squared error (SSE) and the root mean square error (RMSE) were calculated by Eqs. (15), (16) and (17), respectively.

$$R^2 = \frac{\sum q_{i,exp}^2 - SSE}{\sum q_{i,exp}^2} \quad (15)$$

$$SSE = \sum_{i=1}^{N} (q_{i,exp} - q_{i,pred})^2 \quad (16)$$

$$RMSE = \sqrt{\frac{rss}{N_d - P}} \quad (17)$$

where $q_{i,exp}$ and $q_{i,pred}$ represent experimental data and theoretically predicted points, respectively, and rss is the residual sum of squares, N_d is the number of data points, and P is the number of parameters.

In Fig. 8, the CLM predictions are in good agreement with experimental data. As shown in Table 5, the CLM predicted the competitive sorptions successfully (R^2>0.93) except Cs in Sr/Cs system (R^2>0.79). The MELM predictions are also in good agreement with experimental data except Cs in Sr/Cs system. Although SSE and RMSE are low, the MELM predictions (Table 6) are less successful (R^2>0.65) than CLM predictions (Table 5). The synergistic efficiency (θ) of each heavy metal was fitted well to the linear Eq. (6). The positive a and negative b values of Sr in Co/Sr system and Sr/Cs systems and Co in Co/Cs system explain that the θ_i values were negative at low q_j but increased to be positive with q_j, indicating the synergistic effects at above the crossover point ($q_{j,cross}$). In contrast, the θ_i values for Sr in Co/Sr and Cs in Co/Cs systems were positive at low q_j but decreased to be negative with q_j, indicating antagonistic effects (Table 6). As summarized in Table 7, the P-factor model predictions were also less satisfactory (R^2>0.66) than CLM predictions. This is because this model is based on the Langmuir model and it does not consider the interactions and competitions that can influence the sorption capacity, thus, some deviations of the predicted curves from the experimental data are observed [17].

In summary, the sorptions of Co, Sr and Cs onto SAMMS were highly dependent on the properties of both the metals and the sorbent. The physical properties of the studied metals, including electronegativity, softness, ionic radius and hydrolysis constant may affect metals sorption. The correlation between metal properties and its removal capacity by SAMMS seemed to be even more important than the sorbent properties [24].

4. Effect of pH

The effect of initial solution pH on the sorption and precipitation of Co, Sr and Cs is plotted in Fig. 9. For Co (Fig. 9), the sorption capacity of Co is stable at the pH range of 4-8, indicating a possible ion-exchange sorption mechanism. At lower initial solution pH (pH< 4), the sorption of Co^{2+} is suppressed by the excessive presence of H^+ which compete for available active sites with Co^{2+}. This is common in acidic environment when metal ions sorbed onto sorbent. After pH 8, the precipitation of Co resulted in 98% of disappearance of Co^{2+} in solution, not the real sorption onto SAMMS.

In general, the sorption capacity of Sr onto SAMMS increased with pH (Fig. 9). The contribution of precipitation of Sr^{2+} to the total removal of Sr^{2+} from aqueous solution was negligible except for at pH 12. At lower pH (pH=2), the sorption of Sr^{2+} was inhibited in the acidic solution due to the presence of H^+ ion that compete for sorption sites with Sr^{2+}. At the pH range of 3-10, the uptake of Sr^{2+} increased slightly with increase in pH value due to the increase of surface negative charge. The final pH was around pH_{pzc} value of SAMMS (6.5) indicating a possible reaction with sorption sites:

$$\equiv Si\text{-}OH + Sr^{2+} + H_2O \Leftrightarrow S\text{-}OSrOH + 2H^+ \quad (18)$$

$$\equiv Si\text{-}OH + Sr^{2+} \Leftrightarrow \equiv Si\text{-}OSr^+ + H^+ \quad (19)$$

$$\equiv Si\text{-}O^- + Sr^{2+} \Leftrightarrow \equiv Si\text{-}OSr^+ \quad (20)$$

Table 6. Modified extended Langmuir model (MELM) parameters for bi-solute competitive sorption

Binary system	Metals	a	b	$q_{j,cross}$	θ_i at $q_j > q_{j,cross}$	R^2	SSE	RMSE
Co/Sr	Co	−5.4827	0.4091	0.0746	Antagonistic	0.658	0.097	0.104
	Sr	0.9127	−0.3325	0.3643	Synergistic	0.895	0.001	0.012
Sr/Cs	Sr	0.9000	−0.5390	0.5988	Synergistic	0.703	0.042	0.068
	Cs	-	-	-	-	-	-	-
Co/Cs	Co	4.6975	−1.2518	0.2664	Synergistic	0.770	0.073	0.090
	Cs	−3.1998	2.4056	0.7517	Antagonistic	0.940	0.050	0.743

Table 7. P-factor model parameters for bi-solute competitive sorption

Bi-solute system	P_i	R^2	SSE	RMSE
Co/Sr	1.0793/5.2699	0.9756/0.8765	0.0069/0.0015	0.0277/0.0131
Co/Cs	0.6639/3.5764	0.6636/0.7383	0.1063/0.2150	0.1087/0.1545
Sr/Cs	0.9914/1.5010	0.8947/0.7595	0.0149/0.9524	0.0407/0.3253

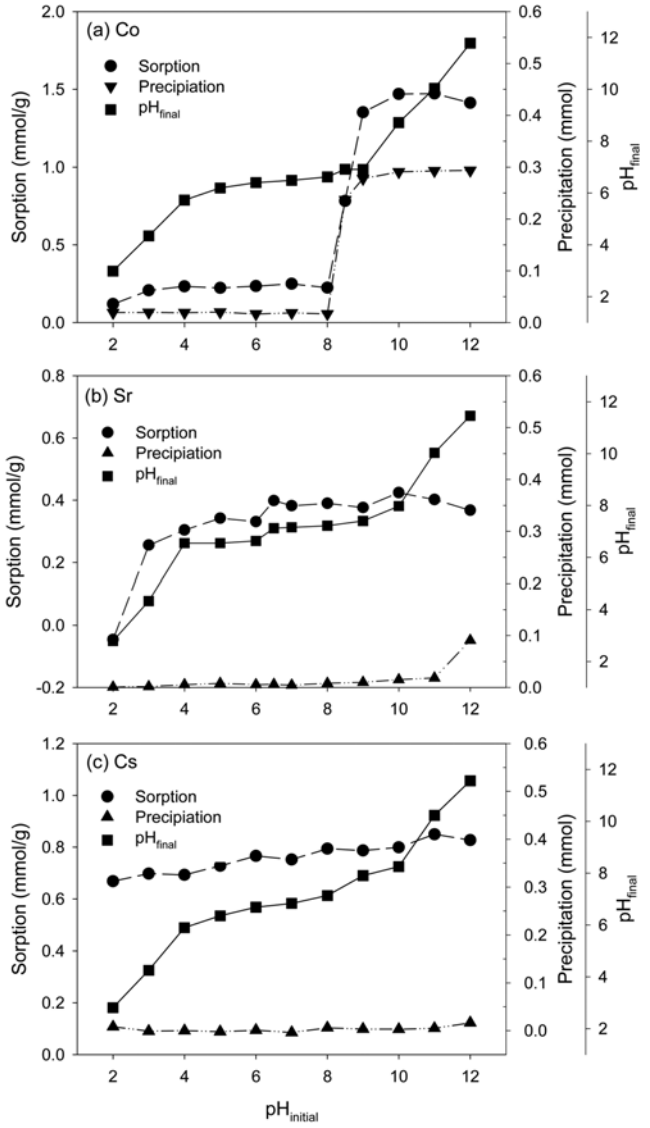

Fig. 9. The influence of initial solution pH on the sorption and precipitation of (a) Co, (b) Sr and (c) Cs onto SAMMS.

After pH 10, the $SrOH^+$ was generated and could not contribute Sr^{2+} removal.

The sorbed amount of Cs onto SAMMS increased slightly (from 0.66 to 0.82 mmol/g) as initial solution pH increased (Fig. 9). The contribution of precipitation of Cs^+ to the total removal of Cs^+ from aqueous solution was negligible. The slight increase of uptake was due to the increase of negative surface charge on SAMMS as initial solution pH increased. The ion exchange was considered as one of the sorption mechanism because of the inherent structure of SAMMS. SAMMS, the synthetic composite material, was sodium copper ferrocyanide immobilized within a mesoporous ceramic matrix functionalized with an ethylenediamine (EDA) terminated silane [1-(2 aminoethyl)-3-aminopropyl]trimethylsilane [10]. When the metal ion M (monovalent or divalent) reacts with SAMMS, the Na^+ in ion exchange func- tional group will be mainly replaced with metal ion during reaction process as expressed as follows:

$$\text{-N} \equiv \text{C-Fe(CN)}_5\text{-(Na}^+)_x + \text{M}^+$$

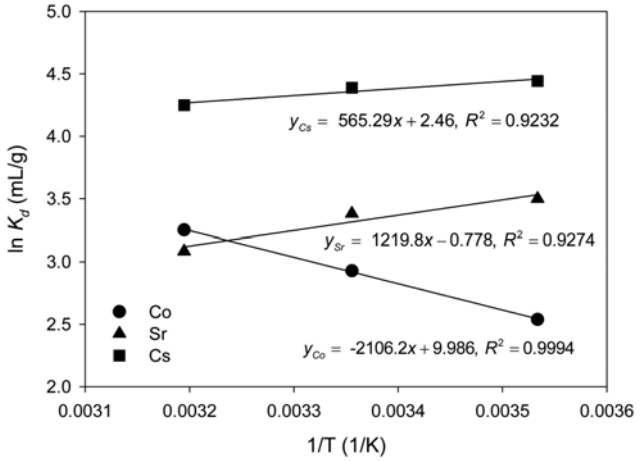

Fig. 10. Relationship between ln K_d and 1/T for Co, Sr and Cs sorption onto SAMMS.

Table 8. Thermodynamic parameters for single-solute sorption of Co, Sr and Cs onto SAMMS

	ΔH^0	ΔS^0	ΔG^0 (kJ/mol)		
	(kJ/mol)	(kJ/mol/K)	283 K	298 K	313 K
Co	17.51	0.083	−5.98	−7.23	−8.47
Sr	−10.14	−0.007	−7.38	−6.63	−5.89
Cs	−4.70	0.020	−10.49	−10.79	−11.10

$$\Rightarrow \text{-N} \equiv \text{C-Fe(CN)}_5\text{-(M}^+)_x + \text{xNa}^+ \quad (21)$$

5. Effect of Temperature

The effect of temperature on the sorption of Co, Sr and Cs onto SAMMS is presented in Fig. 10 and the thermodynamic parameters are listed in Table 8. The sorption capacity of Co increases as temperature increases from 283 K to 313 K, indicating an endothermic sorption process as indicated by the positive ΔH^0 value (17.51 kJ/mol for Co). Thus the sorption of Co has to overcome an activation barrier and increasing temperature favors this reaction [25]. The decrease of sorbed amounts of Sr and Cs with increasing temperature suggests an exothermic sorption reaction as indicated by negative ΔH^0 values for both metals (−10.14 kJ/mol for Sr and −4.70 kJ/mol for Cs, respectively). The magnitude of ΔH^0 was related to the sorption energy, which can explain the type of binding mechanism involved, i.e., physical or chemical sorption. Energies of 4-8 kJ/mol are required by London and van der Waals interactions, compared from 8 to 40 kJ/mol for hydrogen bonding. In contrast, the enthalpy associated with chemical sorption is about 40 kJ/mol [26]. The ΔH^0 values for Sr and Cs sorptions indicated physical sorption, while that of Co sorption indicated complex mechanism combined physical and chemical sorption at this temperature range. In addition, the magnitude of ΔH^0 value for Co sorption was three times higher than that of Cs indicating the dependence of the equilibrium of Cs sorption on temperature was less limited compared to that of Co sorption by SAMMS.

The changes in entropy (ΔS^0) for Co, Sr and Cs were 0.083, −0.007 and 0.02 kJ/mol/K, respectively. The positive values of Co and Cs indicated that the sorption process was accompanied with some struc-

tural changes in the sorbent and sorbate during the sorption reaction [21,27]. Especially, the structural changes in $Cu_x[Fe(CN)_6]$ were accelerated in Co sorption than Cs sorption; sorption occurs mainly by ion exchange with minor structural changes. The negative ΔS^0 value of Sr indicated that the reactions occurred with the decrease in the entropies.

The change of free energy (ΔG^0) for all metals was negative, indicating that the sorption of Co, Sr and Cs onto SAMMS was spontaneous in nature and the degree of spontaneity of the reaction increases with increasing temperature. This may be attributed to increase in the number of active surface sites available for sorption on the sorbent and the decrease in the thickness of the boundary layer surrounding the sorbent with temperature which will accelerate the mass transfer process [22].

CONCLUSIONS

The results of single-solute sorption experiments indicted that SAMMS has potential to remove Co, Sr and Cs from aqueous solution. The sorption data were well fitted with Freundlich, Langmuir, and Dubinin-Radushkevich models. The maximum sorption capacity (q_{mL}) of SAMMS perdicted by Langmuir model was in the order of Cs (1.141 mmol/g)>Co (0.203 mmol/g)≈Sr (0.195 mmol/g). For bi-solute competitive sorptions, the sorption of each metal ion was suppressed by the presence of other metal ion. The maximum sorption capacity (q^*_{mL}) values in bi-solute system were lower than those calculated from single-solute sorption (q_{mL}). The binding energy coefficients (b^*_L) in bi-solute systems were higher than those (b_L) in single-solute sorptions except for Co/Sr system. The CLM, MELM and P-factor model were fitted to the bi-solute competitive sorption. Among these models, CLM fitted the experimental data better than MELM and P-factor model. The sorption of Co onto SAMMS was strongly dependent on pH, while the initial pH slightly affected the sorption of Sr and Cs onto SAMMS. The sorption of Sr and Cs was suppressed by competition with H^+ when the pH was lower than pH_{PZC} (pH 6.5). The positive ΔH^0 value for Co indicated an endothermic sorption process. However, sorptions of Sr and Cs were exothermic (i.e., negative ΔH^0 values). The negative ΔG^0 values indicated all the sorption processes were spontaneous in nature.

ACKNOWLEDGEMENT

This research was supported by Korea Science and Engineering Foundation (KOSEF) grant funded by the Korean government, the Ministry of Education, Science and Technology (grant number: M20706000036-07M0600-03610). The authors would like to acknowledge the Korea Basic Science Institute (Daegu) and Kyungpook National University Center for Scientific Instrument for SEM-EDS and XRD analyses.

REFERENCES

1. J. C. Linehan, C. M. Stiff and G. E. Fryxell, *Inorg. Chem. Commun.*, **9**, 239 (2006).
2. G. E. Fryxell, H. Wu, Y. Lin, W. J. Shaw, J. C. Birnbaum, J. C. Linehan, Z. Nie, K. Kemner and S. Kelly, *J. Mater. Chem.*, **14**, 3356 (2004).
3. G. E. Fryxell, Y. Lin, S. Fiskum, J. C. Birnbaum, H. Wu, K. Kemner and S. Kelly, *Environ. Sci. Technol.*, **39**, 1324 (2005).
4. L. Bois, A. Bonhomme, A. Ribes, B. Pais, G. Raffin and F. Tessier, *Colloids Surfaces A: Physicochem. Eng. Aspects*, **221**, 221 (2003).
5. J. Liu, X. Feng, G. E. Fryxell, L.-Q. Wang, A. Y. Kim and M. Gong, *Adv. Mater.*, **10**, 161 (1998).
6. A. M. Liu, K. Hidajat, S. Kawi and D. Y. Zhao, *Chem. Commun.*, **13**, 1145 (2000).
7. L. Zhang, C. Yu, W. Zhao, Z. Hua, H. Chen and J. Shi, *J. Non-Cryst. Solids*, **353**, 4055 (2007).
8. M. Mureseanu, A. Reiss, I. Stefanescu, E. David, V. Parvulescu, G. Renard and V. Hulea, *Chemosphere*, **73**, 1499 (2008).
9. R. Hanzel and P. Rajac, *J. Radioanal. Nucl. Chem.*, **246**, 607 (2000).
10. Y. Lin, G. E. Fryxell, H. Wu and M. Engelhard, *Environ. Sci. Technol.*, **35**, 3962 (2001).
11. C.-Y. Chang, L.-K. Chau, W.-P. Hu, C.-Y. Wang and J.-H. Liao, *Micropor. Mesopor. Mater.*, **109**, 505 (2008).
12. T. Sangvanich, V. Sukwarotwat, R. J. Wiacek, R. M. Grudzien, G. E. Fryxell, R. S. Addleman, C. Timchalk and W. Yantasee, *J. Hazard. Mater.*, **182**, 225 (2010).
13. D. Wolff-Boenisch and S. J. Traina, *Geochim. Cosmochim. Acta*, **70**, 4356 (2006).
14. A. E. Greenberg, L. S. Clesceri and A. D. Eaton, *Standard Method for the Examination of Water and Wastewater*, 18th Ed., American Public Health Association, Washington, DC, USA (1992).
15. Y. Park, Y.-C. Lee, W. S. Shin and S.-J. Choi, *Chem. Eng. J.*, **162**, 685 (2010).
16. V. C. Srivastava, I. D. Mall and I. M. Mishra, *Chem. Eng. J.*, **117**, 79 (2006).
17. C. Valderrama, J. I. Barios, A. Farran and J. L. Cortina, *Water Air Soil Pollut.*, **210**, 421 (2010).
18. B. Ma, S. Oh, W. S. Shin and S.-J. Choi, *Desalination*, **276**, 336 (2011).
19. J. H. Choi, S. D. Kim, Y. J. Kwon and W. J. Kim, *Micropor. Mesopor. Mater.*, **96**, 157 (2006).
20. K. G. Bhattacharyya and S. S. Gupta, *J. Colloid Interface Sci.*, **310**, 411 (2007).
21. E. I. Unuabonah, K. O. Adebowale and B. I. Olu-Owolabi, *J. Hazard. Mater.*, **144**, 386 (2007).
22. E. Eren, B. Afsin and Y. Onal, *J. Hazard. Mater.*, **161**, 677 (2009).
23. M. A. Raouf, *J. Chem. Technol. Biotechnol.*, **79**, 22 (2004).
24. A. Sdiri, T. Higashi, T. Hatta, F. Jamoussi and N. Tase, *Chem. Eng. J.*, **172**, 37 (2011).
25. E. I. Unuabonah, K. O. Adebowale, B. I. Olu-Owolabi, L. Z. Yang and L. X. Kong, *Hydrometallurgy*, **93**, 1 (2008).
26. I. H. Gubbuk, , *J. Hazard. Mater.*, **186**, 416 (2007).
27. O. Yavuz, Y. Altunkaynak and F. Guzel, *Water Res.*, **37**, 948 (2003).